QUARTERLY OF APPLIED MATHEMATICS

VOLUME LIX DECEMBER · 2001 NUMBER 4

DECEMBER 2001, PAGES 601–614

DYNAMICALLY ACCELERATING CRACKS PART 2: A FINITE LENGTH MODE III CRACK IN ELASTIC MATERIAL

BY

TANYA L. LEISE (*Department of Mathematics, Rose-Hulman Institute of Technology, Terre Haute, IN*)

AND

JAY R. WALTON (*Department of Mathematics, Texas A&M University, College Station, TX*)

Abstract. We consider a dynamically accelerating, finite length, mode III crack in an infinite elastic body. This initial boundary value problem has the nature of a free boundary problem since the crack tip motion is a priori unknown and must be found as part of the solution after imposition of a fracture criterion. Using an analog to a Dirichlet-to-Neumann map, we reduce the fracture problem to integrodifferential equations along the boundary that, for simplicity, we combine with a stress intensity factor fracture criterion. This approach has the advantage of being applicable to cases of multiple cracks as well as, in principle, to mode I cracks and to cracks in viscoelastic materials.

1. Introduction. We extend the methods developed by Walton and Herrmann [12] to a finite length, mode III crack as a first step in a research effort toward developing general methods for dynamic fracture of multiple cracks, mode I cracks, and cracks in viscoelastic solids, with particular attention to simulating the behavior of brittle polymers. For an overview of our long term goals, see [1], [2], and [3]. Building on the operators developed in [12], we can reduce the dynamic elastic fracture problem to integrodifferential operators along the boundary, which for the semi-infinite crack are quite simple in structure. Modifying the semi-infinite crack operators to apply to the case of an asymmetrically growing finite length crack is nontrivial since the crack tip interaction becomes a significant complication; however, once obtained, these operators provide a means of straightforward computation of the displacement and stress along the plane

Received April 21, 1998.

2000 *Mathematics Subject Classification.* Primary 74R15, 45K05; Secondary 74R10.

The authors gratefully acknowledge the support provided for this research from the Air Force Office of Scientific Research under grant number F49620-96-1-0294. This material is also based upon work supported under a National Science Foundation Graduate Research Fellowship.

E-mail address: leise@rose-hulman.edu

E-mail address: jwalton@math.tamu.edu

of the crack. The key difficulty lies in solving for the crack face separation for a given fracture criterion.

Crucial to creating a physically meaningful model is choosing an appropriate fracture criterion. Usually fracture criteria rely on a principle of energy balance, first suggested by Griffith [6]: the crack will propagate if the available energy release rate G equals some required energy release rate γ that is dependent on material properties and crack speed. For example, one would expect very different required energy release rates for a crystalline metal and an amorphous polymer. Determining an appropriate function γ generally requires a micromechanical model specific to the material involved. Such analysis is beyond the scope of this paper, and we will focus on the left-hand side, G, of the energy balance equation. In the quasistatic (elliptic) problem, the function G cannot implicitly limit the crack tip speed; so one must introduce a function γ that does. In the dynamic (hyperbolic) problem, the function G naturally limits the crack speed to the shear wave speed for the mode III problem and to the Rayleigh wave speed in the mode I problem. We will assume that γ is simply constant, which means that only G limits the crack speed; physically, these speeds are too high to be the limiting speeds for most materials; so it will be desirable to improve the fracture criterion eventually. For purposes of illustrating our methods of dealing with G, we will put aside these considerations and choose a stress intensity factor fracture criterion with a constant critical value.

Friedman and Liu [5] have proven existence and regularity theorems in the case of a propagating semi-infinite quasistatic crack in a strip. Since the quasistatic available energy release rate G does not limit crack speed, they introduced the function

$$\gamma = \gamma_0 \frac{v_\infty + v(t)}{v_\infty - v(t)}, \tag{1.1}$$

where $v(t)$ is the crack speed, in order to limit the crack speed to the value v_∞. This required energy release rate is based on elastic-plastic analysis, perhaps not entirely suited to the elastic problem. Another difficulty is that observed crack speeds are too high for the quasistatic equations to be valid. In any case, their method for the quasistatic case cannot be extended to the dynamic (hyperbolic) case since it depends on elliptic regularity estimates.

See [4], [6], [7], [9], and [10] for further discussion of these issues. We will proceed to describe a constructive solution to the dynamic crack problem.

2. The mixed boundary value problem. Consider an antiplane shear crack of finite length in an elastic solid. In the (x, y)-plane, assume that the crack initially lies along $\{-a_0 < x < a_0,\ y = 0\}$. Let $w(x, y, t)$ be the out-of-plane displacement and $\sigma_{23}(x, y, t)$ be the usual shear stress. Apply a load $\sigma_{23}(x, 0, t) = \Lambda(x, t)$ along $-d(t) < x < a(t)$, where $a(t)$ is the position of the right crack tip, $-d(t)$ is the position of the left crack tip, and $\Lambda(x, t)$ is a sufficiently smooth function. See Figure 1. For antiplane deformations, the balance of linear momentum equation becomes the single scalar wave equation

$$w_{tt} = c^2(w_{xx} + w_{yy}) \tag{2.1}$$

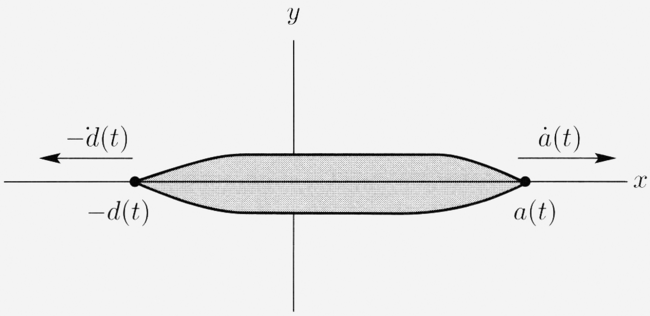

FIG. 1. An accelerating finite length crack

in the upper half (x, y)-plane for $t \geq 0$ with boundary conditions

$$w(x, 0, t) = 0 \quad \text{for } -d(t) > x \text{ or } a(t) < x, \tag{2.2}$$

$$\sigma_{23}(x, 0, t) = \mu w_y(x, 0, t) = \Lambda(x, t) \quad \text{for } -d(t) < x < a(t). \tag{2.3}$$

Here c is the elastic shear wave speed and μ is the elastic shear modulus. We assume a quiescent past with initial conditions $w(x, y, 0) = 0$ and $w_t(x, y, 0) = 0$, and we restrict the speed of the crack tips to be subsonic: $0 \leq \dot{a}(t), \dot{d}(t) < c$. To complete this set of equations, we choose a stress intensity factor fracture criterion: the crack tip at $a(t)$ $(-d(t))$ will propagate only if the stress intensity factor $K_a(t)$ $(K_d(t))$ equals a critical value K_{cr}, where

$$K_a(t) = \lim_{x \to a(t)^+} \left[\sigma(x, t) \sqrt{x - a(t)} \right], \tag{2.4}$$

$$K_d(t) = \lim_{x \to (-d(t))^-} \left[\sigma(x, t) \sqrt{-d(t) - x} \right]. \tag{2.5}$$

Our approach for the finite length crack will be based on the solution method given in [12] for an accelerating, semi-infinite, antiplane shear crack. This same approach can be extended to multiple cracks; moreover, in principle, it can be generalized to include the cases of opening mode cracks and viscoelastic fracture [11]. The method involves modifying the Dirichlet-to-Neumann map for the governing differential equation and combining this new map with an appropriate fracture criterion to solve for the crack tip position functions $a(t)$ and $d(t)$, given a crack face loading $\Lambda(x, t)$.

At this point, it will be convenient to introduce some notation. Define characteristic coordinates $\eta = t + x/c$ and $\xi = t - x/c$ and denote space-time functions in characteristic coordinates via

$$\tilde{f}(\eta, \xi) = f\left(\frac{c}{2}(\eta - \xi), \frac{1}{2}(\eta + \xi) \right).$$

Let $\sigma(x, t) = \sigma_{23}(x, 0, t)$ and $u(x, t) = w(x, 0, t)$.

The Dirichlet-to-Neumann maps for the wave equation (2.1) as developed in [12] and [11] are

$$\tilde{\sigma}(\eta,\xi) = -\frac{2\mu}{c\pi}\frac{\partial}{\partial\eta}\int_{-\xi}^{\eta}\frac{dr}{\sqrt{\eta-r}}\frac{\partial}{\partial\xi}\int_{-r}^{\xi}\tilde{u}(r,q)\frac{dq}{\sqrt{\xi-q}}, \tag{2.6}$$

$$\tilde{\sigma}(\eta,\xi) = -\frac{2\mu}{c\pi}\frac{\partial}{\partial\xi}\int_{-\eta}^{\xi}\frac{dq}{\sqrt{\xi-q}}\frac{\partial}{\partial\eta}\int_{-q}^{\eta}\tilde{u}(r,q)\frac{dr}{\sqrt{\eta-r}}. \tag{2.7}$$

By inverting the Abel operators we find the Neumann-to-Dirichlet maps:

$$\tilde{u}(\eta,\xi) = -\frac{c}{2\pi\mu}\int_{-\eta}^{\xi}\frac{dq}{\sqrt{\xi-q}}\int_{-q}^{\eta}\tilde{\sigma}(r,q)\frac{dr}{\sqrt{\eta-r}}, \tag{2.8}$$

$$\tilde{u}(\eta,\xi) = -\frac{c}{2\pi\mu}\int_{-\xi}^{\eta}\frac{dr}{\sqrt{\eta-r}}\int_{-r}^{\xi}\tilde{\sigma}(r,q)\frac{dq}{\sqrt{\xi-q}}. \tag{2.9}$$

For convenience, we will now consider nondimensionalized equations, using the crack length parameter a_0 as the characteristic length. With magnitudes on the order of 10^{-3} meters for a_0 and 10^3 meters/second for c, we define the nondimensional quantities as follows:

$$x^* = \frac{x}{a_0}, \quad t^* = \frac{ct}{a_0}, \quad \text{and} \quad \sigma^* = \frac{\sigma}{\mu}. \tag{2.10}$$

Note that the characteristic time scale $\tau = \frac{a_0}{c}$ is on the order of 10^{-6} seconds. Experiments can now resolve down to microseconds; so we present simulations on the order of 10-100 time units to observe behavior on the scale of experiments.

In the remainder of this paper, we will drop the asterisks and solely consider the nondimensionalized system. For convenience of notation, introduce retarded and advanced time scales $b_0(t)$ and $b_1(t)$, respectively, corresponding to the right crack tip:

$$b_0(t) = t - a(t), \quad b_1(t) = t + a(t). \tag{2.11}$$

Since we impose subsonic crack propagation ($0 \le \dot{a}(t) < 1$), the functions $b_0(t)$ and $b_1(t)$ will be strictly increasing and hence invertible. These functions will be useful in describing the crack tip path through time when modifying the Dirichlet-to-Neumann maps. Similarly, we introduce time scales for the left crack tip:

$$h_0(t) = t - d(t), \quad h_1(t) = t + d(t). \tag{2.12}$$

In the next sections we tackle the problem of developing an operator that maps known boundary values to unknown and that will enable us as well to solve for the crack tip locations $a(t)$ and $-d(t)$.

3. Solution strategy. As the relations (2.6) and (2.7) stand, to find the stress $\sigma(x,t)$ along the boundary intervals $x < -d(t)$ and $x > a(t)$, where it is unknown, requires full knowledge of the displacement $u(x,t)$ along the boundary, which we do not have. Similarly, using (2.8) and (2.9) to find the displacement along the boundary interval $-d(t) < x < a(t)$, where it is unknown, requires full knowledge of the stress along the boundary, which again we do not have. See Figure 2 for an example of the lightcone that is the region of integration in (2.6)-(2.9), noting the nature of the mixed boundary

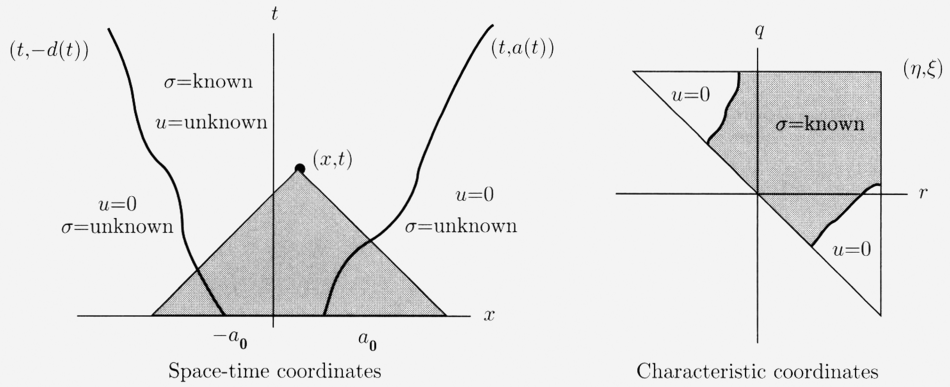

FIG. 2. Lightcone region of integration in the Dirichlet-to-Neumann and Neumann-to-Dirichlet maps

data. The regions containing known data evolve as the crack propagates in an a priori unknown manner. In fact, it is this evolution that we are trying to determine as our final goal.

If there were no left crack tip, we could modify (2.8) as done in [12] by applying the information that $u(x,t)$ vanishes off the crack, then inverting the relation to obtain a modification of (2.9) that requires only the given loading data (2.3). We can do a similar procedure for the finite crack, but the region of integration will still overlap the region where stress in unknown. See Figure 3 for the contrast between the semi-infinite and finite crack problems. To overcome this difficulty, we employ an iterative process. First observe that we can directly use (2.6) to find that the stress $\sigma(x,t)$ vanishes for $\eta < -a_0$ or $\xi < -a_0$. The modified version of (2.6)-(2.9) corresponding to a semi-infinite crack is valid for the finite crack for the regions $-a_0 < \eta < a_0$ and $-a_0 < \xi < a_0$, before any shear stress waves have had enough time to travel from one crack tip to the other (basically, each crack tip acts like the edge of a semi-infinite crack). Once $u(x,t)$ and $\sigma(x,t)$ are determined for these regions, the maps we will develop in Section 4 can be used to determine values for the next strip on which diffracted waves travel back again from one crack tip to the other. This process can be repeated to determine full boundary information in a finite number of steps for any particular time $t > 0$. See Figure 4 for an illustration of these iteration strips.

The procedure for developing the desired maps for a finite crack involves modifying (2.6)-(2.9) by applying boundary condition (2.2) and inverting the resulting Abel operators. The functions $a(t)$ and $d(t)$ are a priori unknown; so we assume arbitrary functions while developing the maps and then use the fracture criterion to determine the crack propagation corresponding to the crack face loading (2.3). In general, we want to be able to determine any value of the stress or the displacement along the boundary that might be needed for application of a fracture criterion. For example, to find the unknown displacement $u(x,t)$ in the region $-d(t) < x < a(t)$, the region of integration in equation (2.6) becomes the intersection of the lightcone as in Figure 2 and the crack face region $-d(t) < x < a(t)$. The resulting relation remains in the form of two Abel operators

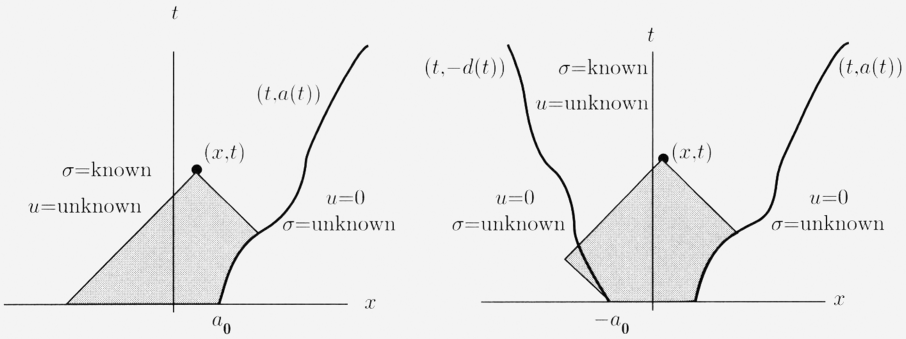

FIG. 3. Regions of integration for maps corresponding to semi-infinite and finite length cracks

that can be inverted to yield an equation giving the displacement in terms of the known loading (2.3) plus the stress in a region where it is unknown, as in Figure 3, necessitating an iteration process as described above. We can also find a similar relation for the stress.

Once we are able to determine full boundary information, we can apply the fracture criterion to solve for the functions $a(t)$ and $d(t)$ that describe the crack propagation resulting from the crack face loading (2.3). For a stress intensity factor criterion, we need to know the coefficient of the square root singularity in the stress at the crack tips. It turns out that the stress intensity factor is easy to deduce from the maps developed for the finite crack and is a function of crack tip speed. Applying the fracture criterion with a constant critical value K_{cr} reduces the problem of finding $a(t)$ and $d(t)$ to a system of ordinary differential equations.

In the next section, we pursue this solution strategy to yield the precise relations needed to calculate the crack propagation.

4. Mappings for a finite crack. To solve the moving interface problem (2.1)-(2.3) along the half-plane boundary, we modify the Dirichlet-to-Neumann map as described in Section 3 so that its evaluation requires only known boundary values. Let $a(t)$ and $d(t)$ be arbitrary (sufficiently smooth) functions satisfying $0 \leq \dot{a}(t), \dot{d}(t) < 1$. We will develop integrodifferential operators that yield the displacement and stress along the boundary corresponding to the crack face loading (2.3). We are unaware of any rigorous proof that this forms a well-posed closed system. Developing such a theory appears to be a highly nontrivial enterprise, and investigation of this point is the subject of ongoing research. Assuming that the problem is well-posed, we develop a constructive method for computing the solution.

We begin by finding a relation to determine unknown values of the displacement along the boundary. For (η, ξ) satisfying $-d(t) < x < a(t)$, apply to (2.6) the fact (2.2) that the displacement vanishes off the crack face:

$$\tilde{\sigma}(\eta,\xi) = -\frac{2}{\pi}\frac{\partial}{\partial\eta}\int_{\max\{-\xi,-a_0\}}^{\eta} \frac{dr}{\sqrt{\eta - r}}\frac{\partial}{\partial\xi}\int_{\max\{-r,b_0\circ b_1^{-1}(r)\}}^{\min\{\xi,h_1\circ h_0^{-1}(r)\}} \tilde{u}(r,q)\frac{dq}{\sqrt{\xi - q}}. \tag{4.1}$$

Fix ξ and invert the outer Abel operator:

$$\int_{\max\{-\xi,-a_0\}}^{\eta} \tilde{\sigma}(r,\xi)\frac{dr}{\sqrt{\eta-r}} = -2\frac{\partial}{\partial\xi}\int_{\max\{-\eta,b_0\circ b_1^{-1}(\eta)\}}^{\xi} \tilde{u}(r,q)\frac{dq}{\sqrt{\xi-q}}. \tag{4.2}$$

Fix η and invert the inner Abel operator:

$$\tilde{u}(\eta,\xi) = -\frac{1}{2\pi}\int_{\max\{-\eta,b_0\circ b_1^{-1}(\eta)\}}^{\xi} \frac{dq}{\sqrt{\xi-q}}\int_{\max\{-q,-a_0\}}^{\eta} \tilde{\sigma}(r,q)\frac{dr}{\sqrt{\eta-r}}. \tag{4.3}$$

This relation holds for (η,ξ) satisfying $-d(t) < x < a(t)$, that is, along the crack face. By starting with equation (2.7), we obtain an alternative map to calculate the displacement along the crack faces:

$$\tilde{u}(\eta,\xi) = -\frac{1}{2\pi}\int_{\max\{-\xi,h_0\circ h_1^{-1}(\xi)\}}^{\eta} \frac{dr}{\sqrt{\eta-r}}\int_{\max\{-r,-a_0\}}^{\xi} \tilde{\sigma}(r,q)\frac{dq}{\sqrt{\xi-q}}. \tag{4.4}$$

Next we want an operator that finds the stress outside the crack face in terms of the given loading (2.3). In particular, for (η,ξ) satisfying $x > a(t)$,

$$\tilde{\sigma}(\eta,\xi) = -\frac{2}{\pi}\frac{\partial}{\partial\eta}\int_{\max\{-\xi,-a_0\}}^{b_1\circ b_0^{-1}(\xi)} \frac{dr}{\sqrt{\eta-r}}\frac{\partial}{\partial\xi}\int_{\max\{-r,b_0\circ b_1^{-1}(r)\}}^{\min\{\xi,h_1\circ h_0^{-1}(r)\}} \tilde{u}(r,q)\frac{dq}{\sqrt{\xi-q}}. \tag{4.5}$$

Substituting equation (4.2) into (4.5) yields

$$\tilde{\sigma}(\eta,\xi) = \frac{1}{\pi}\frac{\partial}{\partial\eta}\int_{\max\{-\xi,-a_0\}}^{b_1\circ b_0^{-1}(\xi)} \frac{dr}{\sqrt{\eta-r}}\int_{\max\{-\xi,-a_0\}}^{r} \tilde{\sigma}(s,\xi)\frac{ds}{\sqrt{r-s}} \tag{4.6}$$

$$= -\frac{1}{\pi}\frac{1}{\sqrt{t-b_0^{-1}(\xi)}}\int_{\max\{0,\frac{\xi-a_0}{2}\}}^{b_0^{-1}(\xi)} \sigma(r-\xi,r)\frac{\sqrt{b_0^{-1}(\xi)-r}}{t-r}dr. \tag{4.7}$$

This relation holds for (η,ξ) satisfying $x > a(t)$, that is, to the right of the crack. Similarly, for (η,ξ) satisfying $x < -d(t)$, we have the relation

$$\tilde{\sigma}(\eta,\xi) = \frac{1}{\pi}\frac{\partial}{\partial\xi}\int_{\max\{-\eta,-a_0\}}^{h_1\circ h_0^{-1}(\eta)} \frac{dq}{\sqrt{\xi-q}}\int_{\max\{-\eta,-a_0\}}^{q} \tilde{\sigma}(\eta,p)\frac{dp}{\sqrt{q-p}} \tag{4.8}$$

$$= -\frac{1}{\pi}\frac{1}{\sqrt{t-h_0^{-1}(\eta)}}\int_{\max\{0,\frac{\eta-a_0}{2}\}}^{h_0^{-1}(\eta)} \sigma(\eta-q,q)\frac{\sqrt{h_0^{-1}(\eta)-q}}{t-q}dq. \tag{4.9}$$

To find the stress intensity factor (2.4), observe that by L'Hôpital's rule,

$$\lim_{x\to a(t)^+}\frac{x-a(t)}{t-b_0^{-1}(\xi)} = 1-\dot{a}(t), \tag{4.10}$$

and take the limits of (4.7) as $x \to a(t)^+$ and of (4.9) as $x \to (-d(t))^-$. We then find that

$$K_a(t) = -\frac{1}{\pi}\sqrt{1-\dot{a}(t)}\int_0^t \sigma(r-b_0(t),r)\frac{dr}{\sqrt{t-r}}, \tag{4.11}$$

$$K_d(t) = -\frac{1}{\pi}\sqrt{1-\dot{d}(t)}\int_0^t \sigma(h_0(t)-r,r)\frac{dr}{\sqrt{t-r}}. \tag{4.12}$$

If the crack were semi-infinite under a load with support in $(-d(t), a(t))$, these equations would be sufficient to directly determine the unknown displacement and stress along the boundary, as well as the stress intensity factor, from the known loading data. For a finite crack, these equations will still be sufficient, but cannot be applied blindly; we must "bootstrap" up to find the unknown boundary values. The relations (4.7) and (4.11) agree with those found by Kostrov [8] for a finite length, antiplane shear crack, but his method of obtaining the results does not seem to extend either to the plane strain case or to viscoelastic materials. Also, Kostrov does not indicate how to extend his result for the finite crack beyond the time it takes stress waves to travel the length of the crack.

The first steps in this "bootstrap" process involve direct applications of (4.9) and (4.7). For clarity of presentation, we will refer to the original crack tip position as a_0 rather than as "1" in the rest of the paper, as this usage suggests the wave fronts associated with the crack tips. If $\xi \le -a_0$ or $\eta \le -a_0$, then $\sigma(x,t) = 0$. If $-a_0 < \xi < a_0$, then we can directly find the unknown displacement and stress as in the semi-infinite crack case:

$$\tilde{u}(\eta,\xi) = -\frac{1}{2\pi}\int_{\max\{-\eta, b_0 \circ b_1^{-1}(\eta)\}}^{\xi} \frac{dq}{\sqrt{\xi - q}} \int_{\max\{-q,-a_0\}}^{\eta} \tilde{\Lambda}(r,q)\frac{dr}{\sqrt{\eta - r}} \tag{4.13}$$

for $x < a(t)$, while we have for $x > a(t)$,

$$\sigma(x,t) = -\frac{1}{\pi}\frac{1}{\sqrt{t - b_0^{-1}(\xi)}} \int_0^{b_0^{-1}(\xi)} \Lambda(r-\xi, r)\frac{\sqrt{b_0^{-1}(\xi) - r}}{t - r}dr. \tag{4.14}$$

Similarly, if $-a_0 < \eta < a_0$, then

$$\tilde{u}(\eta,\xi) = -\frac{1}{2\pi}\int_{\max\{-\xi, h_0 \circ h_1^{-1}(\xi)\}}^{\eta} \frac{dr}{\sqrt{\eta - r}} \int_{\max\{-r,-a_0\}}^{\xi} \tilde{\Lambda}(r,q)\frac{dq}{\sqrt{\xi - q}} \tag{4.15}$$

for $x > -d(t)$, while we have for $x < -d(t)$,

$$\sigma(x,t) = -\frac{1}{\pi}\frac{1}{\sqrt{t - h_0^{-1}(\eta)}} \int_0^{h_0^{-1}(\eta)} \Lambda(\eta - q, q)\frac{\sqrt{h_0^{-1}(\eta) - q}}{t - q}dq. \tag{4.16}$$

The stress $\sigma(x,t)$ is now known in a large enough region for the operators in (4.7) and (4.9) to yield $\sigma(x,t)$ for $a_0 < \eta < b_1 \circ b_0^{-1}(a_0)$ and $a_0 < \xi < h_1 \circ h_0^{-1}(a_0)$, respectively. Once $\sigma(x,t)$ has been determined for some $n \ge 0$ on the regions

$$\eta < (b_1 \circ b_0^{-1} \circ h_1 \circ h_0^{-1})^n(a_0), \tag{4.17}$$

$$\xi < h_1 \circ h_0^{-1} \circ (b_1 \circ b_0^{-1} \circ h_1 \circ h_0^{-1})^n(a_0), \tag{4.18}$$

it can subsequently be computed in the adjacent strips in the following order:

$$(b_1 \circ b_0^{-1} \circ h_1 \circ h_0^{-1})^n(a_0) < \eta < (b_1 \circ b_0^{-1} \circ h_1 \circ h_0^{-1})^{n+1}(a_0), \tag{4.19}$$

$$h_1 \circ h_0^{-1} \circ (b_1 \circ b_0^{-1} \circ h_1 \circ h_0^{-1})^n(a_0) < \xi < h_1 \circ h_0^{-1} \circ (b_1 \circ b_0^{-1} \circ h_1 \circ h_0^{-1})^{n+1}(a_0). \tag{4.20}$$

Each strip will have height parallel to the t-axis of at least $2a_0$; so any value $\sigma(x,t)$ can be computed in a finite number of steps. See Figure 4.

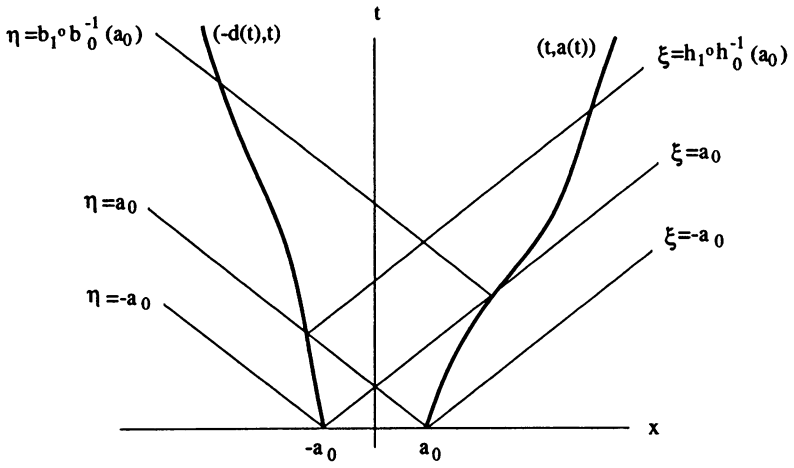

FIG. 4. Bootstrapping strips for iterative calculation of the stress and displacement along the x-axis

Thus far we assumed arbitrary functions $a(t)$ and $d(t)$. Next we apply the iterative procedure to these operators to solve the inverse problem of determining the functions $a(t)$ and $d(t)$ corresponding to the chosen fracture criterion. To determine the right crack tip position $a(t)$, we apply the fracture criterion: $\dot{a}(t) = 0$ if $|K_a(t)| < K_{\rm cr}$; otherwise $0 \le \dot{a}(t) < c$ and $|K_a(t)| = K_{\rm cr}$. Apply an analogous criterion to the left crack tip. The system now simplifies to two ordinary differential equations:

$$\dot{a}(t) = \begin{cases} 0 & \text{if } |K_a(t)| < K_{\rm cr}, \\ 1 - \left(\frac{\pi K_{\rm cr}}{\int_0^t \sigma(r - b_0(t), r) \frac{dr}{\sqrt{t-r}}} \right)^2 & \text{if } |K_a(t)| = K_{\rm cr}, \end{cases} \tag{4.21}$$

$$\dot{d}(t) = \begin{cases} 0 & \text{if } |K_d(t)| < K_{\rm cr}, \\ 1 - \left(\frac{\pi K_{\rm cr}}{\int_0^t \sigma(h_0(t) - r, r) \frac{dr}{\sqrt{t-r}}} \right)^2 & \text{if } |K_d(t)| = K_{\rm cr}. \end{cases} \tag{4.22}$$

so that given $\Lambda(x,t)$, it is straightforward to compute the crack tip position functions $a(t)$ and $d(t)$.

5. Example: fixed constant load. To illustrate application of these mappings, consider an accelerating crack under a fixed constant load

$$\Lambda(x,t) = \begin{cases} -\sigma_0 & \text{if } -a_0 \le x \le a_0, \\ 0 & \text{if } a_0 < |x| < a(t), \end{cases} \tag{5.1}$$

for which the crack will propagate symmetrically: $d(t) = a(t)$. As discussed in [4], we expect to observe dynamic overshoot of the stress intensity factor. Before the first "crack tip interaction," the stress intensity factor $K(t)$ increases; after this point, $K(t)$ will decrease during the next time interval, after which it may oscillate (the terms corresponding to each successive iterative strip alternate in sign).

The time at which information from one accelerating crack tip first reaches the other crack tip (that is, accelerating in the opposite direction) will be $t = b_0^{-1}(a_0)$. For $t \in [0, b_0^{-1}(a_0)]$, the stress intensity factor is exactly the same as for a semi-infinite crack:

$$K_a(t) = \frac{2\sigma_0}{\pi}\sqrt{1-\dot{a}(t)}\left(\sqrt{t} - \sqrt{a(t)-a_0}\right). \tag{5.2}$$

The crack will begin to propagate at time

$$t_0 = \left(\frac{K_{\rm cr}\pi}{2\sigma_0}\right)^2 \quad \text{if } \sigma_0 \geq \frac{K_{\rm cr}\pi}{2\sqrt{2a_0}}; \tag{5.3}$$

otherwise the crack will remain stationary. $K(t)$ is strictly increasing on the interval $(0, \min\{t_0, b_0^{-1}(a_0)\})$, then remains constant with value $K_{\rm cr}$ until time $t = b_0^{-1}(a_0)$; the crack cannot arrest until after this first time interval.

The crack behavior will diverge from that of the semi-infinite case after this first crack tip interaction. The stress intensity factor for $t > b_0^{-1}(a_0)$ for a semi-infinite crack with faces along $x < a(t)$ under the loading (5.1), and traction-free on the remaining crack face, will be

$$K_{\rm si}(t) = \frac{2\sigma_0}{\pi}\sqrt{1-\dot{a}(t)}\left(\sqrt{a(t)+a_0} - \sqrt{a(t)-a_0}\right). \tag{5.4}$$

Once the crack arrests, $K_{\rm si}(t)$ will remain constant with value $K_{\rm cr}$. For the finite length crack, the effect of the crack tip interaction appears as an additional term:

$$K_a(t) = K_{\rm si}(t) - \frac{1}{\pi}\sqrt{1-\dot{a}(t)}\int_{(b_0(t)-a_0)/2}^{b_1^{-1}\circ b_0(t)} \sigma(r-b_0(t), r)\frac{dr}{\sqrt{t-r}}. \tag{5.5}$$

Even after crack arrest, this additional term will continue to change, unlike the first term. In general, the stress intensity factor will decrease on $[b_0^{-1}(a_0), b_0^{-1} \circ b_1 \circ b_0^{-1}(a_0)]$, after which it may oscillate. (See Figure 5.)

Comparing the quasistatic and dynamic behavior of the semi-infinite and finite cracks further illustrates the effect of crack tip interaction. Note that the semi-infinite crack case can be considered an approximation for the finite length crack in which we disregard the presence of a second crack tip. The quasistatic stress intensity factor for the semi-infinite crack is the same as in the dynamic case but without the term $\sqrt{1-\dot{a}(t)}$. The quasistatic stress intensity factor for the finite length crack under the loading (5.1) is

$$K_{\rm qs}(t) = \frac{\sigma_0\sqrt{2a(t)}}{\pi}\arcsin\frac{a_0}{a(t)}. \tag{5.6}$$

The quasistatic model predicts that if $\sigma_0 < K_{\rm cr}\sqrt{2/a_0}$ the crack will remain stationary, while the dynamic model predicts that if $\sigma_0 < \pi K_{\rm cr}/\sqrt{2a_0}$ the crack will remain stationary. If the applied load is great enough to force the crack to propagate, the quasistatic estimate of the final crack length a_f satisfies

$$\pi K_{\rm cr} = \sigma_0\sqrt{2a_f}\arcsin\frac{a_0}{a_f}, \tag{5.7}$$

while the estimate for a dynamically acclerating semi-infinite crack is

$$a_f = a_0 + \left(\frac{a_0}{C} - \frac{C}{2}\right)^2, \quad \text{where } C = \frac{\pi K_{\rm cr}}{2\sigma_0}. \tag{5.8}$$

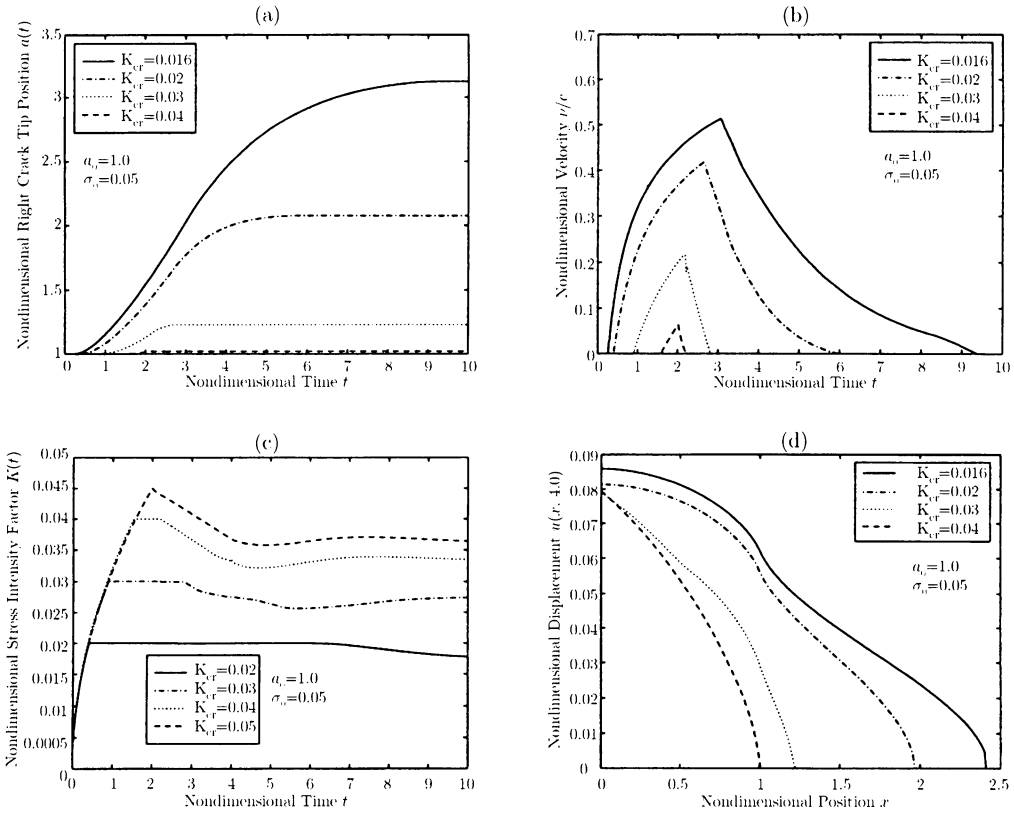

FIG. 5. Propagation of a finite crack under a constant fixed load: (a) Crack tip paths under a constant fixed load; (b) Crack tip velocities under a constant fixed load; (c) Stress intensity factors under a constant fixed load; (d) Crack face profile at time $t = 4.0$ under a constant fixed load

The dynamic values for a_f are much greater than those predicted by the quasistatic model, but less than those predicted for a semi-infinite crack (for which the quasistatic and dynamic predictions agree). See Figure 6 for a comparison of these three cases.

6. Example: constant load on entire crack face. As another simple example, consider an accelerating crack under a constant load on the entire crack face:

$$\Lambda(x,t) = -\sigma_0 \quad \text{if } -a(t) < x < a(t), \tag{6.1}$$

for which the crack will again propagate symmetrically: $d(t) = a(t)$. As before, the crack will remain stationary if $\sigma_0 < \pi K_{\rm cr}/\sqrt{2a_0}$; otherwise, the crack will begin to propagate at time $t_0 = (\frac{\pi K_{\rm cr}}{2\sigma_0})^2$. For $t \in [0, b_0^{-1}(a_0)]$,

$$K_a(t) = \frac{2\sigma_0\sqrt{t}}{\pi}\sqrt{1-\dot{a}(t)}. \tag{6.2}$$

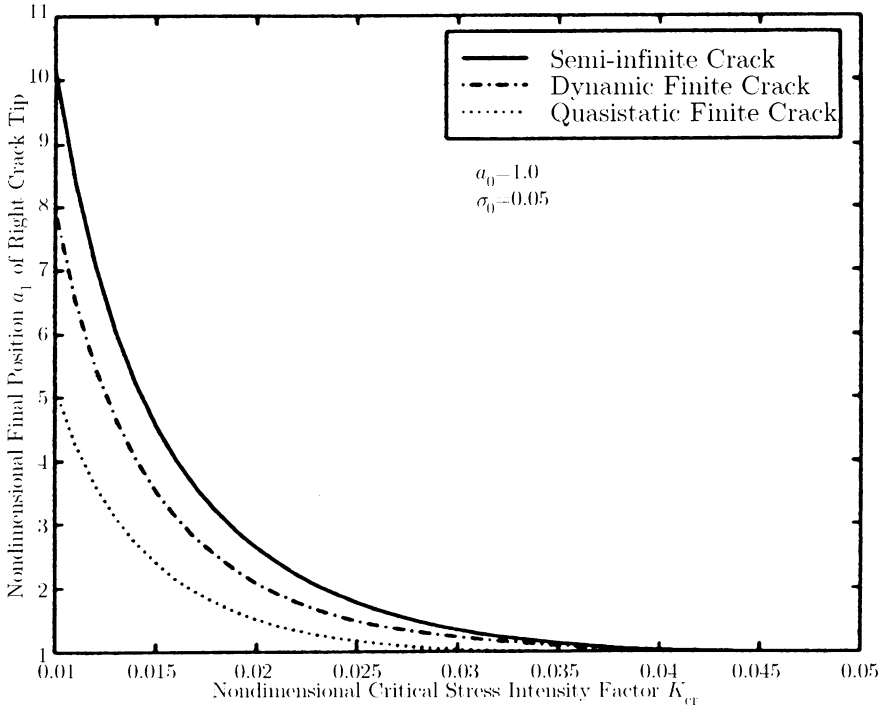

FIG. 6. Comparison of final crack length predictions

For $t > b_0^{-1}(a_0)$, we can write the stress intensity factor as was done in the previous example:

$$K_{\rm si}(t) = \frac{2\sigma_0}{\pi}\sqrt{1-\dot{a}(t)}\sqrt{t - b_1^{-1} \circ b_0(t)}, \tag{6.3}$$

$$K_a(t) = K_{\rm si}(t) - \frac{1}{\pi}\sqrt{1-\dot{a}(t)} \int_{(b_0(t)-a_0)/2}^{b_1^{-1}\circ b_0(t)} \sigma(r - b_0(t), r)\frac{dr}{t-r}. \tag{6.4}$$

If the crack propagates, it will have velocity $\dot{a}(t) = 1 - t_0/t$ for t in the interval $[t_0, t_0 \exp(2a_0/t_0 - 1)]$. After this time interval, the presence of the second crack tip may cause the stress intensity factor to oscillate, so that the crack may arrest, arrest and start again, or accelerate to the limiting speed as a semi-infinite crack would. See Figure 7 for examples of these behaviors.

7. Conclusion. The goal in this and succeeding papers is to reduce initial boundary value problems for dynamic, accelerating cracks to integrodifferential equations that are amenable to computation, coupled with a fracture criterion. One of the advantages of this method lies in its potential applicability to more general material behavior, such as in viscoelastic materials. The problem of choosing a physically appropriate fracture criterion is highly material dependent and is an issue that will be dealt with separately.

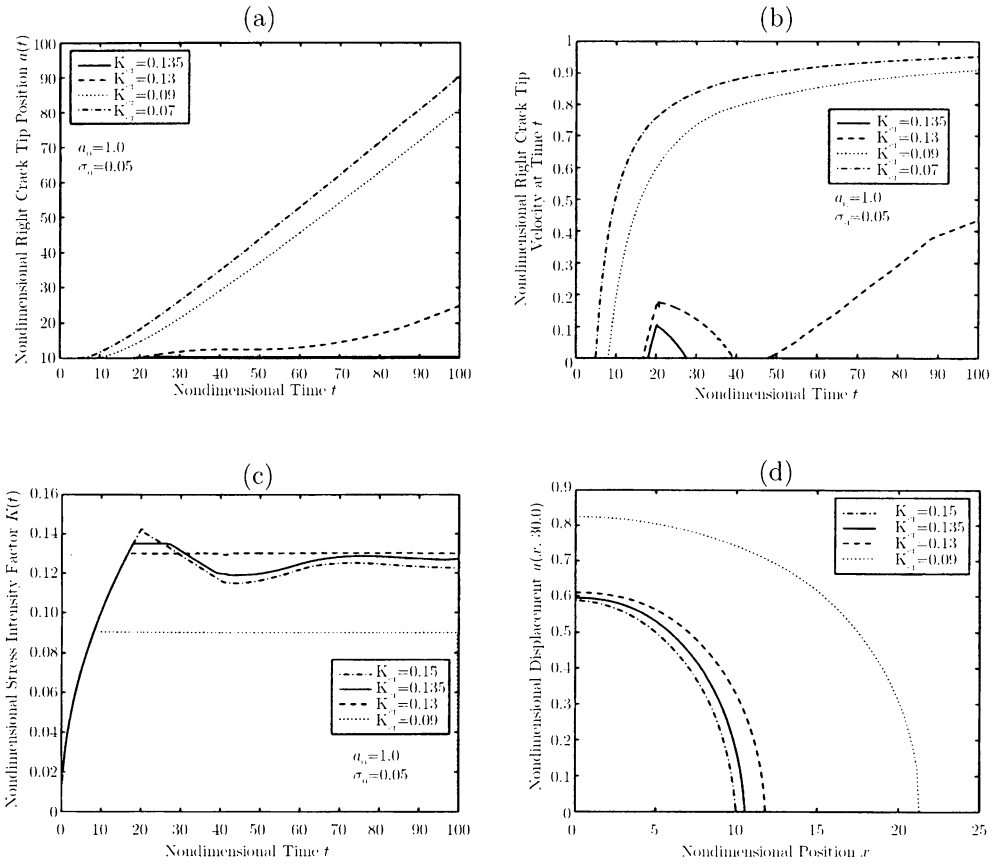

FIG. 7. Propagation of a finite crack under a constant load on the entire crack face: (a) Crack tip paths under constant load on entire crack face; (b) Crack tip velocities under constant load on entire crack face; (c) Stress intensity factors under constant load on entire crack faces; (d) Crack face profile at time $t = 30.0$ under constant load on entire crack face

REFERENCES

[1] F. Costanzo and J. R. Walton, *A study of dynamic crack growth in elastic materials using a cohesive zone model*, Internat. J. Engrg. Sci. **35**, 1085–1114 (1997)

[2] F. Costanzo and J. R. Walton, *A numerical solution technique for a class of integro-differential equations in elastodynamic crack propagation problems*, Comp. Meth. Appl. Mech. Engrg. **162**, 19–48 (1998)

[3] F. Costanzo and J. R. Walton, *Numerical simulations of a dynamically propagating crack with a nonlinear cohesive zone*, Internat. J. Frac. **91**, 373–389 (1999)

[4] L. B. Freund, *Dynamic Fracture Mechanics*, Cambridge University Press, Cambridge, 1990

[5] Avner Friedman and Yong Liu, *Propagation of cracks in elastic media*, Arch. Rat. Mech. Anal. **136**, 235–290 (1996)

[6] A. A. Griffith, *The phenomenon of rupture and flow in solids*, Philos. Trans. Royal Soc. London **A221**, 163–198 (1920)

[7] M. E. Gurtin, *On the energy release rate in quasi-static elastic crack propagation*, J. Elasticity **9**, 187–195 (1979)

[8] B. V. Kostrov, *Unsteady propagation of longitudinal shear cracks*, Appl. Math. Mech. (PPM) **30**, 1042–1049 (1966)

[9] J. L. Rice, *Mathematical analysis in mechanics of fracture*, Fracture, Vol. 2 (H. Liebowitz, ed.), Academic Press, 1968, pp. 191–311

[10] L. I. Slepyan, *Principal of maximum energy dissipation rate in crack dynamics*, J. Mech. Phys. Solids **41**, 1019–1033 (1993)

[11] J. R. Walton, *Dynamic viscoelastic fracture*, Crack and Contact Problems for Viscoelastic Bodies (G.A.C. Graham and J. R. Walton, eds.), CISM Courses and Lectures No. 356, Springer-Verlag, Wien and New York, 1995, pp. 259–311

[12] J. R. Walton and J. M. Herrmann, *A new method for solving dynamically accelerating crack problems: part 1. The case of a semi-infinite mode III crack in elastic material revisited*, Quart. Appl. Math. **50**, 373–387 (1992)